Adsorbent in bioremediation of crude oil polluted environment: influence of physicochemical characteristics of various saw dusts

***Ukpaka CP and Edwin Ibiso**

Department of Chemical, Petrochemical Engineering, Rivers State University of Science and Technology, P.M.B. 5080 Nkpolu-Port Harcourt, Rivers State, Nigeria.

Abstract

The study of the effect of physicochemical parameters of various sawdusts on the bioremediation of crude oil polluted water environment was carried out to determine the level of adsorption rate of crude oil in water bodies. Various particle size of sawdust were used 0.5 mm, 1.18 mm, 2.80 mm, 3.35 mm and 6.30 mm and the rate of adsorption in order of magnitude is 6.30 mm > 3.35 mm > 2.80 mm >1.18 mm > 0.5 mm for palm tree <mango < bamboo sawdust as revealed in the research work. The results obtained revealed that moisture content influence the rate of adsorption of the crude oil as well as microbial activity for the various samples studied. The microorganisms present in the different sawdust's were isolated and identified as Bacillus species with total bacteria count of 1.60 x 10^6 cell/ml, 1.28 x 10^6 cell/ml and 1.4 x 10^6 cell/ml for mango, bamboo and palm tree sawdust. The experimental data obtained from the research was used in simulating the developed mathematical model which leads to the computation of the specific rate of adsorption and the determination of the maximum specific rate of adsorption and the equilibrium rate of the system. These were achieved by the application of LineWeaver Burk plot principle and findings indicate that all the various sawdust used for the studies are capable of enhancing bioremediation of polluted environment in both surface and underground water (salt water river and underground water from tap) were sampled for this research work.

Keywords: Adsorbent, bioremediation, crude oil, sawdust, environment, physicochemical.

INTRODUCTION

The environmental impact of crude oil exploration, exploitation, production and processing has been gradually acknowledge as a major problem in the economic development of oil producing communities in Nigeria. Oil pollution on soil and water environment has become a major problem due to toxicity of the substance on the vegetation. Different approach has been applied to enhance remediation of polluted soil and water environment. Initially, chemical methods have been used but currently biological method is commonly used due to the environment friendly of the end result achieved.

The research work is following the trend of bioremediation in which the physicochemical characteristics of the various sawdusts was tested as a way forward to determine its contribution speeding up the bioremediation of crude oil contaminated environment. This research will entail the analysis of physiochemical parameters of the various sawdusts in terms of: pH, bulk density, pore volume, conductivity, porosity, particle size, bacteria level, moisture content and organic carbon as well as the influence of these functional parameters in the adsorption rate of the various sawdusts in crude oil. Mathematical model was developed in this paper to examine the adsorption rate of the various sawdusts used for the research work.

The sawdust samples used for the studies were classified as soft, semi hard and hard wood sawdust with different physicochemical characteristics concentration as presented in the paper and the effect of the parameters (functional parameters) were discussed and its significance to the research work was highlighted in terms of bioremediation.

Bioremediation is one of the best method of cleaning polluted environment, either soil or water environment as

presented by various research groups (Omokaro and Remesh, 2009; Omoaghe, 2003 and Ukpaka, 2010). The functional parameters of the various sawdusts and the degradation rate of the substrate, in which the activity of the micro-organism is greatly inhibited as a result of change in concentration of the crude oil was reported by Onifade, Abubaka and Ekundayo, (2007).

The soft, semi-hard and hard wood sawdust used for this research work was collected in Niger Delta area of Nigeria. Although, several research works has been done by using, sawdust in bioremediation of polluted site as reported by Ukpaka, 2008, 2009 and 2010.

Bioremediation of areas degradated by pollutions or otherwise are impacted through mismanagement of ecosystem is a form of biotechnological approach aimed at rehabilitating the area for positive uses. Most of the restoration of Polycyclic Aromatic Hydrocarbons (PAH) contaminated sites depends on the activities of bacteria (microbial degradation) *like pseudomona aerugilosa* or use of plant (phytoremediation) or use of fungi (mycoremediation) (Kishor et al., 2011; Nwufo, 1997; Obidiolayide et al., 2010; Ogoni, 2001; Onwuru, 1999).

There is need for bioremediation because crude oil spills may cause oil damage to the environment in many ways. Oil spill on land may lead to retardation of vegetation growth and cause soil infertility (Chaineau, Yepremian, Vidalie and Ballerini, 2003).

The physiochemical parameters of sawdust will enables us understand the nature and selectivity of different adsorbents and comparing their properties against others. Cleaning and adsorption of commercial oil spills cost so much money. Sometimes, unpredictable weather hampers the cleaning of oil spills. If there is a heavy storm, it would be impossible to clean up the oil spill in that particular period of time.

Bioremediation is a process of using living organisms to remedy environmental problems such as contaminated soil and water, some micro-organisms in the soil and water naturally feed on some hazardous substance certain chemicals that are harmful to people and the environment. The activities of the micro-organisms help in changing some of the hazardous substance into water and harmless gases such as carbon (IV) oxide. Plants sources (sawdust) can be used to clean up soil and water environment as presented by Chorom, (2010).

Owing to the problems associated with physical, mechanical and chemical methods, involved in bioremediation of polluted land there is need for a safer and less expensive approach to remediation of polluted environments using sawdusts.

MATERIALS AND METHODS

Sample collection

Sawdust samples were collected from Buguma sawmill, in Asari-Toru Local Government of Rivers State, Nigeria. It was transported to the Chemical/Petrochemical Engineering laboratory and microbiology laboratory, in Rivers State University of Science and Technology, Port Harcourt, Rivers State, Nigeria for onward analysis.

Salt water was collected from eagle Island River in Port-Harcourt, Port-Harcourt Local Government Area in Rivers State of Nigeria. Underground water (tap water) was collected from the existing borehole in area of laboratory of Chemical/Petrochemical Engineering and transferred into the main laboratory for analysis. Crude oil was gotten from Port Harcourt Refinery, Eleme, in Rivers State of Nigeria.

Equipment and materials used

Materials and Apparatus: The following equipments and materials were used during the investigation: standard laboratory coat; various sorbent (sawdust), boombas sawdust (soft wood), palm tree sawdust (semi-hardwood), mango sawdust (hardwood), crude oil, salt water, tap water (underground water), sieve, batch reactor, working table, retort stand, thermometer, and polyethylene.

Experimental procedure

The experiment was conducted by considering the following procedures, batch reactor containing 1000ml (1 liter) of salt and tap water were collected as states above and a constant temperature of 30^0C was maintained in various batch reactors as well as using three (3) different types of sawdust and the sawdust acts as the adsorbent. 50ml of crude oil was introduced into the different batch reactors containing the salt and tap (underground) water and sawdust of 25g of sieve sized of 0.5mm, 1.18mm, 2.80mm, 3.35mm, and 6.3mm was inoculated in the batch reactors and the system was allowed for period of 1 to 5 day. In each day one reactor of the experimental set-up was harvested for both salt and tap water media and the results obtained recorded.

During the investigation precaution was taken to prevent crude oil from diffusing into the bottom of the reactor by the application of polyethylene as illustrated in the main diagram of the experimental set-up. Each of the batch bioreactor reactors was stirred daily to ensure proper mixing of the adsorbent with contaminant as well as to facilitate the rate of adsorption in the system.

Polyethylene material was introduced to prevent adsorption diffusing into the water environment, but only have contact with the crude and the sawdust (sorbent); thermometer was also inserted into the reactor to check the temperature level; after introducing the polyethylene material into the reactor to fetch the crude oil and the sawdust, the remaining water was weighed and the

results recorded. The rate of adsorption in this process was determined as well as which of the sawdust will be more effective for bioremediation of crude oil polluted water environment. The crude oil samples obtained from the decantation process was separated from the sawdust using a solvent from the aromatic group such as benzene, ethane, acetone and chloroform.

During the process the oil is being absorbed by the sawdust decantation process follows which, the crude oil extraction from the sawdust for further use. The extracted crude oil and the sawdust are useful in the society such as: production of animal feeds as well as agricultural purpose, composed manure (agricultural purpose) in place of industrial fertilizer, fire starter, and electricity

Adsorption analysis method

This was carried out using a batch reactor, a known weight (2kg) was added to the solution of crude oil with initial solution of crude oil with initial concentration of 25mg/L; and the sawdust sample was collected from Buguma saw mill, and was transported to the laboratory of Chemical Engineering Department, Rivers State University of Science and Technology, Port Harcourt, Rives State, Nigeria. The samples were stored in a dried oven at a temperature of 70^0c for 12 hours and the dried sawdust was collected from the oven, cooled and sieved with the use of number of different sieve size as presented in this paper and the product of the sieving was used to examine the adsorption test of the various sawdust on the crude oil.

Physiochemical analysis method

Elemental analysis

In this part of the experiment, elements such as organic carbon were analyzed using the necessary equipment. The equipment used was elemental analyzer equipped with an inductive furnace analyzer (CCE instrument), the CE instrument is used for the conductivity. After elemental analysis other physiochemical properties of the sawdust such as particle size, bulk density, pore volume, porosity, moisture content, conductivity, bacteria level such as the isolation, identification and the characterization and pH content were determined.

Particle size analysis

Particle size distribution values were determined by saving with a mesh size of 8, 4, 2, 1, 0, 0.5, 0.25 and 0.09mm saturation capacity was conducted according to the weight.

The electrical conductivity was determined using EC meter and caution exchange was determined by the method sodium acetic, whereas the sawdust particles size distributions were analyzed using hydrometer method.

Thirty grams of air-dried sawdust was weighed and sieved with a 2mm sieve and transferred to a “mill shaker” mix cup. Cup of 5% calgon (dispersing agent) was added to the sawdust sample and the sawdust sample with the dispersing agent was stirred for 15 minutes. The suspension was transferred to the glass measuring cylinder. Distilled water was added to increase the volume to 100cm^3 marks. The content was shaken thoroughly and then place on a flat surface and the time taken. Immediately, a hydrometer was inserted into the suspension and, the first reading on the hydrometer was taken after 40 seconds. The hydrometer was recovered and the temperature recorded with a thermometer. The suspension was allowed to stand while other readings were taken at the appropriate time percentage of the various particle sizes were computed from the reading.

pH Content Analysis

Sawdust pH was measured using a pH meter. Twenty grams of air dried sawdust was weighed
and sieved with a 2mm sieve and transferred into 100ml beaker. 5ml of distilled water was added to and stirred occasionally for 30 minutes with a glass rod. The electrode of a standardized pH meter inserted into it and the sawdust pH in water was measured when the digital display reading was stable. The result was reported as pH measured in water using 1:2:5 sawdust to water ratio.

Organic carbon concentration analysis

This was determined as follows: five grams of sample was weighed and sieved with 0.5mm sieve, this was done in duplicate before being transferred to 25ml Erlyen flash, 10ml of 1W($k_2Cr_20_7$) solution was pipetted into each flask and was stirred gently to disperse the sawdust. This was followed by the addition of 25ml concentrated H_2S0_4 using a graduated cylinder taking a few seconds only in the operation. The flask was stirred gently until sawdust and reagents were mixed vigorously for one minute to affect more complete oxidation and allowed to stand for 30minutes. The contents were diluted with distilled water of about 100ml with 5% coolgen as well addition of 5ml of orthophosphoric acid was mixed with 5ml of Barium chloride which was introduced into the flask. One part of the solution was Titrate against 0.4N ferrous Ammonium sulphate until a change in colour from thick violet to light green was

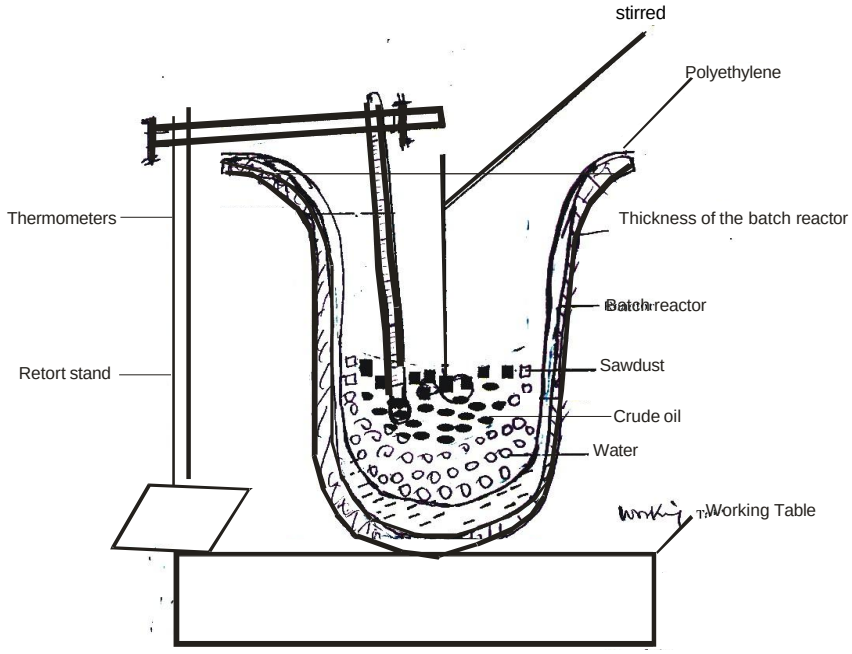

Figure 1a. Experimental set up to investigate the rate of adsorption using various sawdusts in crude oil contaminated environment

observed.

Bulk density

The empty centrifuge tube was weighed and result recorded as well as filling the samples up to the brim of the centrifuge tube, then tap tube 25 times such that the sample will come down to 10mL volume and them weigh the tube and the sample.

$$Bulk\ \ Density\ (g) \quad = \frac{Mass\ of\ \ sawdust}{volume\ of\ \ sawdust}$$

Pore volume

$$Pore\ volume\ (g) \quad = \frac{Increasein\ weight}{Density\ of\ water\ (H_2O)}$$

Porosity analysis

Porosity (f) was computed from bulk density value thus:

$$porosity\ \ (\%) \ = \ \frac{Pore\ volume}{Total\ \ volume} \quad x\ \ 100$$

Bacteria level analysis

The following procedures were applied in terms of isolation, identification and characterization of the various bacteria in the sawdust as stated below:

- 1gram of sawdust was dissolved in 9ml of sterile H_2O and 0.1mL was collected using a sterile automatic pipe and was placed on a nutrient agar, and spread using a spreader, and it was incubated at 37^{o}C for 24 hours (1day)
- The cultures were examined macroscopically for the morphological characteristics and examined for their motility. The grain reaction, coagulate and catalyze tests were carried respectively. To identify the isolated bacteria and the results are as recorded.

The model formulation

The model

The model was developed considering the experimental set up of a batch system as presented in Figure 1a. The following assumptions were taken for the development of the model in this research work, which includes:

a. A batch process was considered
b. Different sawdust was used in the investigation to ascertain the rate of adsorption
c. The reaction was stirred daily for 5 days
d. The consideration of point c is very important since it is one of the major factors that influence the rate of adsorption of crude oil in aqueous medium
e. Polyethylene material is introduced to prevent adsorption diffusing into the water environment but only

have contact with crude oil, detailed as presented in the Figure 1a above.

Model formulation

Considering the material balance of the batch bioreactor, thus,

$$\begin{bmatrix}\text{Input into the}\\ \text{control volume}\end{bmatrix} = \begin{bmatrix}\text{output from the}\\ \text{control volume}\end{bmatrix} \pm \begin{bmatrix}\text{The rate of disapprance}\\ \text{due to chemical reactor}\\ \text{within thecontrol volume}\end{bmatrix} + \begin{bmatrix}\text{The rate of accumulation}\\ \text{within thecontrol volume}\end{bmatrix} \quad (1a)$$

In a batch reactor input = output and is equal to zero, therefore equation (a) become

$$\begin{bmatrix}\text{The rate of accumulation}\\ \text{within the control value}\end{bmatrix} = \begin{bmatrix}\text{The rate of disapprance}\\ \text{due to chemical reactor}\\ \text{within the control volume}\end{bmatrix} \quad (1b)$$

where

$$\text{The rate of accumulation within the contorl volume} = \frac{\text{dm}}{\text{dt}} \quad (1c)$$

$$\text{The rate of disapprance due to chemical reaction within the control volume} = \beta m \quad (1d)$$

Therefore substituting equation (1c) and (1d) into equation (1b) we have

$$\frac{dm}{dt} = \beta m \quad (1e)$$

Where β = proportionality constant

m = concentration of the adsorbent

$\frac{dm}{dt}$ = change in concentration of adsorbent per unit time.

The mathematical model was developed based on some principles governing the rate of adsorption of contaminants using solid materials as presented in this research work. The equation presented in equation (1) was formulated using the following concept. Considering that the rate of adsorption of the contaminant is proportional to the rate of change of the system with respect to time, therefore.

$$\frac{dm}{dt} = \beta m \quad (1)$$

Equation (1) can be rearranged to give

$$\frac{dm}{m} = \beta dt \quad (2)$$

$$\int_{m_0}^{m} \frac{dm}{m} = \beta \int_0^t dt \quad (3)$$

$$\left[In\, m\right]_{m_0}^{m} = \beta \left[t\right]_0^t \quad (4)$$

Simplifying equation (4) we have

$$In\ m - In\ m_0 = \beta\left[t - 0\right] \quad (5)$$

$$In \frac{m}{m_0} = \beta\ t \quad (6)$$

Taking the log of the both sides of equation (6), we have

$$m = m_o e^{\beta t} \quad (7)$$

Equation (7) can be written as:

$$\beta = \frac{1}{t} In \frac{m}{m_o} \quad (8)$$

Substituting the expression of equation (8) into equation (7) we have;

$$m = m_0\ e^{\left(\frac{1}{t} in \frac{m}{m_0}\right)t} \quad (9)$$

Equation (9) is accepted when the proportionality constant is positive or increasing. Equation (7) defines the change in concentration of adsorbent with respect to increase in the functional parameter of interest. But when a decrease in the functional parameters of interest is obtained, the differential expression to define the mathematical concept is given as:-

$$\frac{dm}{dt} = -\beta m \quad (10)$$

Applying the necessary mathematical tools into equation (10) we have

$$\beta = -\frac{1}{t} In \frac{m}{m_0} \quad (11)$$

and

$$m = m^0\ \ell^{-\beta t} \quad (12)$$

Substituting $\beta = \frac{1}{t} In \frac{m}{m_0}$ into equation (12), we have

$$m = m_o\ e^{\left(-\frac{1}{t} In \frac{m}{m_0}\right)t} \quad (13)$$

Equation (13), will be used when there is decrease in the proportionality constant (β) or negative.

Michael menten's model

Recalling the first order general equation of the Michael Menten's model mathematically, we have

$$R = \frac{R_{\max}[S]}{k_s + [S]} \quad (14)$$

Considering when R =m, that the specific rate of adsorption, therefore equation (14) can be written as

$$m = \frac{m_{\max} \cdot [S]}{k_s + [S]} \quad (15)$$

where

$$m = m_0\, e^{\beta t} = m_0\, e^{\frac{1}{t}\, In^{\frac{m}{m_o}}}$$ Therefore equation (15) can be expressed as:-

$$m_0\, e^{\beta t} = \frac{[m_0\, e^{\beta t}]_{\max} [S]}{k_s + [S]} \quad (16)$$

Substituting the expression of β into equation (16), thus

$\beta = \frac{1}{t} In \frac{m}{m_o}$ into equation (16), we have

$$m_0\, e^{\left(\frac{1}{t} In \frac{m}{m_0}\right)} = \frac{\left[m_0\, e^{\left(\frac{1}{t} In \frac{m}{m_0}\right)}\right]_{\max} [S]}{k_s + [S]} \quad (17)$$

Equation (17) defines the rate of adsorption in terms of increase in proportionality constantβ.
But in terms of decrease in the proportionality constant β we have the given expression in equation (18) as shown below.

$$m_0\, e^{-\frac{1}{t}\left(In \frac{m}{m_0}\right)} = \frac{\left[m_o\, e^{-\frac{1}{t}\left(In \frac{m}{m_0}\right)}\right]_{\max} [S]}{K_s + [S]} \quad (18)$$

Model for inhibiting parameter

pH inhibiting factor

In this case pH was considered as one of the major factor that inhibits or facilitate the rate of bio-adsorption as well the chemical composition of the substrate. Mathematical expression was formulated in relationship with the Michael Menten's equation was as a way forward to evaluate the inhibiting factor of pH in the bioadsorption of crude oil in a batch bioreactor in different aqueous media. The Michael Menten model was expressed in relationship to the various aqueous media (salt water and tap or underground water). As presented in the equation below:

$$\frac{R \max[s]}{ks + [s]} \quad (19)$$

In term of pH as an inhibitor we have;

$$R = \frac{R_{\max}[s]}{k_s + [s]} \cdot pH \quad (20)$$

Considering the rate of change of pH as a function of time dependent in a batch reactor process and recall-principle governing equation (1e) and expressing pH mathematically, we have the expression below when an increase in pH values are obtained:

$$\therefore \quad \frac{dpH}{dt} = rpH \quad (21)$$

But considering when a decrease in pH favors the reaction, the differential equation can be written as follows.

$$\frac{dpH}{dt} = -rpH \quad (22)$$

The general solution to equation (21) and (22) can be written as follows:

$$(pH)_t = (pH) e_o^{rt} \quad (23)$$

This is achieved by using the following boundary condition at

$$\left\{\begin{matrix} t = 0, & t = t \\ pH = 0,\ pH_{(0)} = (pH)_0 & \end{matrix}\right\} \quad (23a)$$

Equation (23) can be used for increase in pH using the same boundary conditions as stated in equation (23a) we have

$$(pH)_t = (pH)_0\, e^{-rt} \quad (24)$$

Equation (24) can expressed as

$$r = -\frac{1}{t} \ln \frac{pH}{(pH)_O} \quad (25)$$

Equation (25) can be written as

$$r = \frac{1}{t} in \frac{pH}{(pH)_O}$$ *for increase in* pH *concentration* (26)

Equation (26) can be related to the Michael Menten's equation as presented in equation (23) when substituted into equation (20) and rearranging we have

$$R = \frac{R_{\max}[S]}{K_S + [S]} (pH)_o\, e^{rt} \quad (27)$$

In terms of the developed model for increase in pH concentration we have

$$m_o \ell^{rt} = \frac{[m_o \ell^{rt}]_{\max} [s]}{ks + [s]} (pH)_o\, e^{rt} \quad (28)$$

In terms of the developed model for decrease in pH concentration

$$m_o\, e^{-rt} = \frac{[m_o \ell^{-rt}]_{\max} [s]}{ks + [s]} (pH)_o\, e^{-rt} \quad (29)$$

where

$$r = \frac{1}{t} In \frac{pH}{(pH)_O}$$

Substituting the value of r into equation (29), we have:

$$R = \frac{R_{\max}[S]}{K_S + [S]} (pH)_o e^{\left(\frac{1}{t} In \frac{pH}{pH}\right)t} \quad (30)$$

$$m_o e^{-rt} = \frac{[m_o e^{-rt}][S]}{K_S + [S]_{\max}} (pH)_o e^{\left(\frac{1}{t} In \frac{pH}{pH}\right)t} \quad (31)$$

For

$$r = -\frac{1}{t} in \frac{pH}{(pH)_O}$$

Equation (30) and (31), can be written as follows

$$R = \frac{R_{\max}[S]}{K_S + [S]} (pH)_o e^{\left(\frac{-1}{\tau} In \frac{pH}{pH_o}\right)t} \quad (32)$$

$$m_o e^{-rt} = \frac{[m_o e^{-rt}][S]}{K_S + [S]_{\max}} (pH)_o e^{\left(\frac{-1}{t} In \frac{pH}{(pH)_0}\right)t} \quad (33)$$

Porosity model as an inhibitor

The mathematical model in terms of change in concentration of porosity can be expressed in conjunction with Michael Menten's equation as defined below:

$$R = \frac{R_{\max}[S]}{k_s + [S]} . porosity \quad (34)$$

Considering the rate of change of porosity as a function of time, therefore the mathematical expression when related to equation (1b) can be written as

$$\frac{dporosity}{dt} = \lambda\ porosity \quad \textit{for increase in porosity concentration} \quad (35)$$

and

$$\frac{d\ porosity}{dt} = -\lambda\ porosity \quad \textit{for decrease in porosity concentration} \quad (36)$$

Using the following boundary conditions at porosity = 0, porosity (0) = $(porosity)_0$, therefore the general solution for equation (35) and (36) can be written as:

$$(porosity)_t = (porosity)_o e^{\lambda t} \quad (37)$$

$$(porosity)_t = (porosity)_o e^{\lambda t} \quad (38)$$

Equation (38) can be written as;

$$\lambda = \frac{1}{t} In \frac{porosity}{(porosity)_o} \quad \textit{for decrease in porosity concentration} \quad (39)$$

Similarly, equation (35) can be written as;

$$\lambda = \frac{1}{t} In \frac{porosity}{(porosity)_o} \quad \textit{for increase in porosity concentration} \quad (40)$$

Equation (36) can be related to the Michael Menten's equation, in terms of correlation with porosity inhibiting as (34) presented in equation (41).

$$R = \frac{R_{\max}[S]}{k_s [S]} . porosity \quad (41)$$

In terms of Michael's Menten's model for increase in porosity concentration we have

$$R = \frac{R_{\max}[S]}{k_s [S]} . (porosity)_0 e^{\lambda t} \quad (42)$$

In terms of the developed model for increase in porosity concentration, we have

$$m_o e^{-\lambda t} = \frac{[m_0 e^{-\lambda t}][S]}{k_s + [S]_{\max}} . (porosity)_0 e^{-\lambda t} \quad (43)$$

In terms of the developed model for decrease in porosity concentration

$$m_o e^{-\lambda t} = \frac{[m_0 e^{-\lambda t}][S]}{k_s + [S]_{\max}} . (porosity)_0 e^{-\lambda t} \quad (44)$$

where

$$\lambda = \frac{1}{t} In \frac{porosity}{(porosity)_0}$$

Substituting the value of λ into equation (43), and (44), we have the following expression;

$$R = \frac{R_{\max}[S]}{k_s [S]} . (porosity)_0 e^{\left(\frac{1}{t} In \frac{porosity}{(porosity)_0}\right)t} \quad (45)$$

$$m_o e^{-\lambda t} = \frac{[m_0 e^{-\lambda t}][S]}{k_s + [S]_{\max}} . (porosity)_0 e^{\left(\frac{1}{t} In \frac{porosity}{(porosity)_0}\right)t} \quad (46)$$

$$for\ \lambda = -\frac{1}{t} In \frac{porosity}{(porosity)_o} \quad (47)$$

Similarly, substituting equation (46a) into equation (41) we have (41) and (39)

$$R = \frac{R_{\max}[S]}{k_s + [S]} . (porosity)_0 e^{\left(-\frac{1}{t} In \frac{porosity}{(porosity)_0}\right)t} \quad (48)$$

and further simplification yields:

$$m_o e^{-\lambda t} = \frac{[m_0 e^{-\lambda t}][S]}{k_s + [S]_{\max}} . (porosity)_0 e^{\left(\frac{1}{-\tau} In \frac{porosity}{(porosity)_o}\right)t} \quad (49)$$

where

[S] = Hydrocarbon substrate concentration

K_s = Michael menten's constant

R_{max} = Rate of reaction

Table 1. Experimental analysis result on the rate of adsorption of various particle size of mango sawdust in salt water for different days

Particle Size (mm)	Adsorption Concentration (%)				
	Day 1	Day 2	Day 3	Day 4	Day 5
0.05mm	9.34	9.41	9.45	9.49	9.55
1.18mm	9.60	9.70	9.99	10.01	10.30
2.80m	10.4	10.21	10.31	10.37	10.44
3.35mm	10.48	10.66	10.68	11.70	11.76
6.30mm	12.18	12.25	12.30	12.35	12.47

Table 2. Experimental analysis result on the rate of adsorption of various particle size of palm sawdust in salt water in salt water for different days

Particle Size (mm)	Adsorption Concentration (%)				
	Day 1	Day 2	Day 3	Day 4	Day 5
0.05mm	9.60	9.80	10.10	10.20	10.25
1.18mm	10.30	10.67	10.44	10.47	10.49
2.80m	10.50	10.51	11.53	11.55	11.56
3.35mm	11.68	11.41	11.54	11.55	11.59
6.30mm	11.61	11.63	11.65	11.70	11.71

Table 3. Experimental analysis result on the rate of adsorption of various particle size of boombas sawdust in salt water for different days

Particle Size (mm)	Adsorption Concentration (%)				
	Day 1	Day 2	Day 3	Day 4	Day 5
0.05mm	18.90	18.95	18.75	18.80	18.90
1.18mm	19.22	19.35	11.58	19.59	19.61
2.80m	19.62	19.63	19.68	19.70	19.72
3.35mm	19.73	19.83	19.81	19.83	19.84
6.30mm	19.85	19.86	19.88	19.89	19.92

RESULTS AND DISCUSSION

The results obtained from the investigation are presented in Figures and Tables as shown below:

The results presented in Table 1 illustrate the adsorption concentration of mango sawdust immersed in salt water medium upon the influence of time and particle size diameter. From Table 1, it is seen that adsorption rate increases with increase in time, in all cases of particle size diameter. The variation on the adsorption concentration of the mango sawdust immersed in salt water medium can be attributed to the variation in time as well as the particle size diameter. Other factors that may influence the rate of adsorption of mango sawdust as presented in Table 1 are the physicochemical parameters.

Results of Table 2 illustrate the variation on the adsorption concentration of palm sawdust upon the variation in time as well as the particle size diameter. The trend on the variation of the adsorption concentration of palm sawdust is similarly to that of mango sawdust, this can be attributed to the closest to the physicochemical parameters value as shown in this paper (Table 7). Increase in adsorption concentration was observed with increase in time as well as increase in particle size diameter as presented in Table 2.

Table 3 illustrates the experimental analysis results on the rate of adsorption of boombas sawdust upon the influence of time and particle size diameter. Increase in adsorption concentration of boombas sawdust immersed in salt water medium was observed with increase in time as well as particle size diameter. The results obtained indicate a variation on the adsorption concentration of boombas immersed in salt water with variation in time and particle size diameter. The variation on the adsorption concentration of boombas sawdust can be attributed to the variation in the physicochemical parameter of the system as well as other environmental factors.

Increase in days of exposure of the bioadsorption

Table 4. Experimental analysis result on the rate of adsorption of various particle size of mango sawdust in underground water (tap water) for different days

Particle Size (mm)	Adsorption Concentration (%)				
	Day 1	Day 2	Day 3	Day 4	Day 5
0.05mm	11.60	11.84	11.85	11.86	11.87
1.18mm	11.88	11.89	11.91	11.95	11.98
2.80m	11.99	12.10	12.24	12.25	11.26
3.35mm	12.27	12.33	12.36	12.68	12.69
6.30mm	12.40	12.42	12.44	12.50	12.52

Table 5. Experimental analysis result on the rate of adsorption of various particle size of palm sawdust in water for different days

Particle Size (mm)	Adsorption Concentration (%)				
	Day 1	Day 2	Day 3	Day 4	Day 5
0.05mm	8.80	8.82	8.84	83.85	8.87
1.18mm	8.89	8.92	8.95	8.96	8.98
2.80m	9.97	9.99	10.02	10.04	10.07
3.35mm	10.10	10.12	10.15	10.18	10.19
6.30mm	10.20	10.25	10.28	10.30	10.37

Table 6. Experimental analysis result on the rate of adsorption of various particle size of boombas sawdust in underground water (tap water) for different days

Particle Size (mm)	Adsorption Concentration (%)				
	Day 1	Day 2	Day 3	Day 4	Day 5
0.05mm	20.60	20.64	20.71	20.72	20.74
1.18mm	20.75	20.77	20.78	20.79	20.82
2.80m	20.84	20.86	20.89	20.90	20.91
3.35mm	20.94	20.96	21.99	22.04	20.10
6.30mm	22.22	22.23	22.40	22.51	20.55

reactor set up, yielded increase in adsorption concentration of mango sawdust in batch reactor upon the influence of time and particle size diameter as presented in Table 4. Increase in adsorption concentration of mango sawdust was observed with increase in time and particle size diameter. The variation in the adsorption concentration of mango sawdust immersed in underground or tap water medium can be attributed to variation in time and particle size.

Analysis result on the rate of adsorption of underground or tap water upon the influence of particle size and time is presented in Table 5. Increase in adsorption concentration of palm sawdust immersed in underground or tap water medium was observed to increase with increase in particle size diameter and time as presented in Table 5. The variation on the concentration can be attributed to the variation on the physicochemical parameters of sawdust, crude oil, water medium and other environmental factors.

Table 6 illustrates the experimental analysis result of boombas sawdust subjected into an aqueous medium containing crude oil and underground or tap water for a period of time. An increase in the adsorption concentration was observed with increase in time and particle size. The variation on the adsorption concentration can be attributed to the variation on the physicochemical parameters and other environmental factors.

Table 7 illustrates the various physicochemical parameters of the various component used for this investigation in the following order of mangnitude: porosity (%) palm sawdust > mango sawdust > boombas sawdust, pH: boombas > mango > palm dust (alkaline in nature), bacteria level (cell/ml): boombas > mango > palm dust, bulk density (g): mango sawdust > palm sawdust > boombas sawdust pore volume (g): palm

Table 7. Experimental analysis result on the physiochemical parameters of the various sawdust used

Physiochemical Parameters	Mango sawdust	Palm sawdust	Boombas sawdust
Porosity (g)	0.14	0.15	0.13
pH	8.10	7.95	8.14
Bacteria level (cell/ml)	1.6×10^6	1.47×10^6	2.8×10^6
Bulk Density (g)	3.1	1.36	1.19
Pore volume (g)	0.0143	0.15	0.013
Organic carbon	2.6	3.6	1.3
Moisture content (%)	20	10	30
Particle size (g)	20	61	21
Conductivity (μs)	547	1828	215

Table 8. Experimental analysis result on the characterization of bacteria level types of bacillus species isolated and identified

Morphology	Characteristic of Bacillus species				
	Motility	Grain reaction	Catalazes	Coagulaze	Possible isolate
1. White entire 1mm dry surface non-mucoid colonies	+	+	+	-	Bacillus species
2. Creamy entire dry colonies	+	+	+	-	Bacillus species

Table 9. Experimental analysis result on the total bacteria count

Sawdust(Samples)	Total Bacteria count(cell/ml)	Identified bacteria
Mango sawdust	1.60×10^6	Bacillus species
Boombas sawdust	1.28×10^6	Bacillus species
Palm tree sawdust	1.47×10^6	Bacillus species

Note: Grain strain = grain positive rods

sawdust < mango sawdust > boombas sawdust > organic carbon: palm sawdust > mango sawdust > palm sawdust, moisture content (%): boombas sawdust < mango sawdust < palm sawdust and conductivity (μs): palm sawdust > mango sawdust > boombas sawdust as presented in Table 7.

Bacterial level, thus include: isolation, identification, and characterization.

The results presented in Table 8 illustrates the experimental analysis result on the characterization of bacteria level isolated and identified in the three samples of the sawdust namely mango, sawdust, palm sawdust and boombas in terms of the morphology as well as the characterization of bacillus species defined or sampled in terms of motility, grain reaction, calalazes, coagulate and possible isolation and identification as presented in Table 8. The positive sign (+) indicate presented and negative sing (-) indicate absent in comparison in two concept of morphology.

Results presented in Table 9, illustrates the experimental analysis result on the total bacteria count of the various sawdusts studied. The order of magnitude in terms of total bacteria count (cell/ml) is mango sawdust > palm sawdust > boombas sawdust and microorganisms isolated and identified is bacillus species as presented in this paper.

From Figure 1 it is seen that the coefficient of the rate of adsorption $\frac{1}{moe^{-rt}}$ increased within 15 to 26% at the coefficient of the substrate within 0.105 to 0.106 and attain a constant value at the range of >0.106 and later decrease in increase in coefficient of substrate (reciprocal of substrate). The cure presented in Figure 1 does not follow the principle of LineWeaver Burk plot. Therefore the specific rate of adsorption and the equilibrium constant of the system can not be established.

Table 10, illustrates the computation results to estimate the specific rate of adsorption and coefficient of adsorption (reciprocal of specific rate of adsorption) upon the influence of time and particle size diameter. Decrease in the rate of adsorption (m_oe^{-rt}) was observed with increase in time at particle size of 0.5mm in salt water medium. Increase in functional coefficient of adsorption or reciprocal of functional coefficient within time range of 2 to 3 days was and suddenly observed remain constant within time range of 3 to 4 days and later decrease with increase in time.

Figure 2 illustrate the graph of adsorption rate of

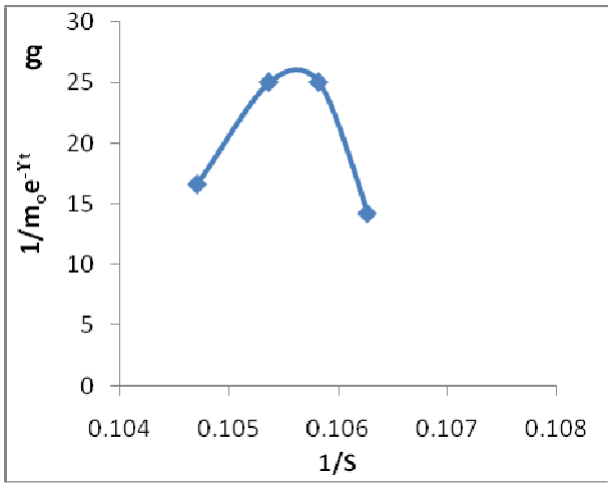

Figure 1. Graph of reciprocal of maximum adsorption rate of particle size (0.5mm) for mango sawdust of particle in salt water against reciprocal of substrate concentration

Table 10. Rate of adsorption for mango sawdust of particle size 0.5mm in salt water

Time (day)	Substrate [S]	1/Substrate [S]	Rate of adsorption m_oe^{-rt}	Coefficient of adsorption m_oe^{-rt}
1	9.34	0.107066381	-	-
2	9.41	0.106269926	0.07	14.2857143
3	9.45	0.105820106	0.04	25
4	9.49	0.105374078	0.04	25
5	9.55	0.104712042	0.06	16.6666667

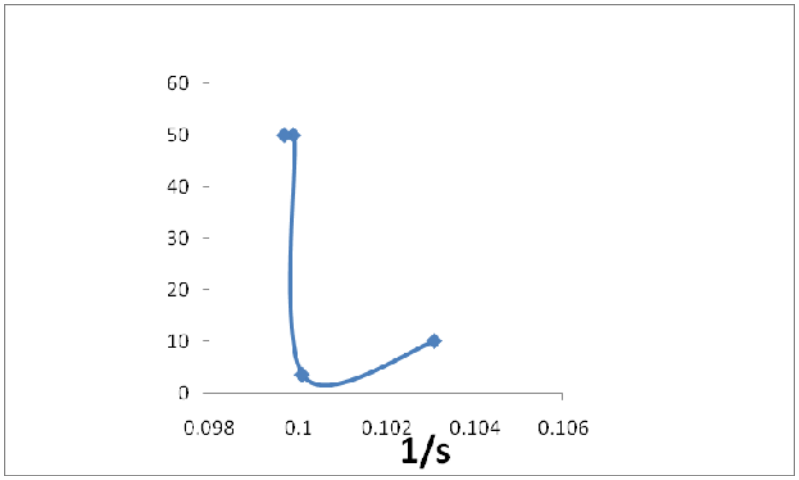

Figure 2. Graph of reciprocal of maximum adsorption rate of particle size (1.18mm) adsorption for mango sawdust in salt water against days

particle size obtained from mango sawdust upon the influence of coefficient of the substrate (reciprocal of the substrate). The curve obtained cannot be used to establish the LineWeaver Burk plot because it does not obey the rate. Increase in reciprocal of the rate of adsorption was observed at the initial time before sudden decrease as presented in Figure 2.

Table 11, illustrates the rate of adsorption for mango sawdust of particle size 1.18mm in salt water. Mathematical computation was applied in evaluating the

Table 11. Rate of adsorption for mango sawdust of particle size 1.18mm in salt water

Day	Substrate (S)	1/ Substrate [S]	Rate of adsorption m_oe^{-rt}	Coefficient of adsorption $1/m_oe^{-rt}$ (g/day)$^{-1}$
1	9.6	0.104166667	-	-
2	9.7	0.103092784	0.1	10
3	9.99	0.1001001	0.29	3.448275862
4	10.01	0.0999001	0.02	50
5	10.03	0.099700897	0.02	50

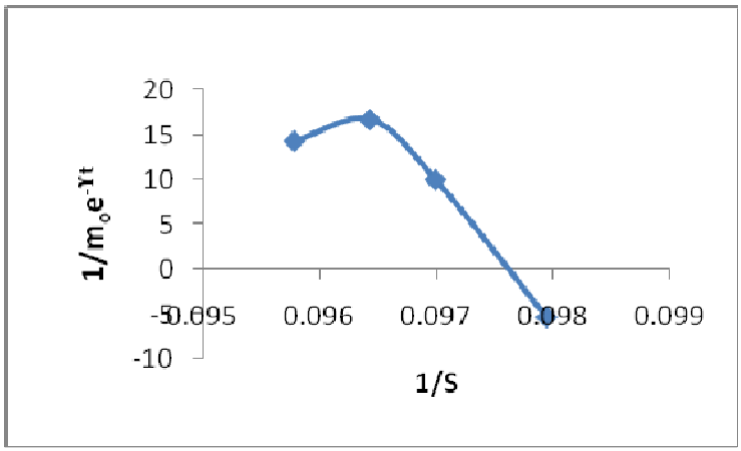

Figure 3. Graph of reciprocal of maximum adsorption rate of particle size (2.80mm) for mango sawdust in salt water against reciprocal of substrate concentration

Table 12. Rate of adsorption for mango sawdust of particle size 2.80mm in salt water

Day	Substrate (S)	1/ Substrate [S]	Rate of adsorption m_oe^{-rt} (g/day)	Coefficient of adsorption $1/m_oe^{-rt}$ (g/day)$^{-1}$
1	10.4	0.096153846	-	-
2	10.21	0.097943193	-0.19	-5.263157895
3	10.31	0.09699321	0.1	10
4	10.37	0.096432015	0.06	16.66666667
5	10.44	0.095785441	0.07	14.28571429

experimental data obtained to establish the determination of the specific rate of adsorption and functional coefficient of specific rate of adsorption or the reciprocal of specific rate of adsorption. The determined values are useful in establish the LineWeaver Burk plot as presented by Michael Mente's equation. The Michael Menten equation is found useful to the determination of maximum specific rate of adsorption as well as the equilibrium or disassociation constant of the process. In this case the specific rate of adsorption (Moe^{-r}) increased within 2 to 3 days and later decrease with a constant value of 0.2 whereas the coefficient of adsorption $\left(\frac{1}{moe^{-rt}}\right)$ decrease from 2 to 3 day and also increase with a constant value of 50 (g/day)$^{-1}$.

The result presented in Figure 3 illustrates the relationship between the reciprocal of the specific rate of adsorption and the reciprocal of the substrate. A slight increase in reciprocal of the specific rate was observed with increase in the reciprocal of the substrate within the range of 15.0 to 17.5(g/day)$^{-1}$ for $1/Moe^{-rt}$ and 0.096 to 0.0965g^{-1}. the maximum specific rate of adsorption and the equilibrium constant on the rate of adsorption can not be establish since the curve obtained does not obey the LineWeaver Burk plot model, therefore $[Moe^{-rt}]_{max} = K_S$ = not possible as presented in Figure 3.

The rate of adsorption for mango sawdust upon the influence of particle size 2.80mm in salt water medium is presented in Table 12. The result present decrease in substrate concentration from day 1 to day 2 and increase from day 5 to days whereas the specific rate of

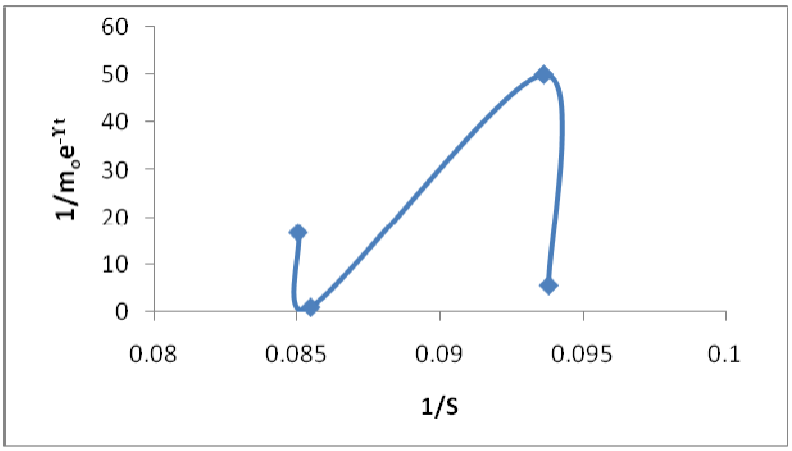

Figure 4. Graph of reciprocal of maximum adsorption rate of particle size (3.35) for mango sawdust in salt water against

Table 13. Rate of adsorption for mango sawdust of particle size 3.35mm in salt water

Day	Substrate(S)	1/ Substrate [S]	Rate of adsorption m_oe^{-rt} (g/day)	Coefficient of adsorption $1/m_oe^{-rt}$ $(g/day)^{-1}$
1	10.48	0.095419847	-	-
2	10.66	0.09380863	0.18	5.555555556
3	10.68	0.093632959	0.02	50
4	11.7	0.085470085	1.02	0.980392157
5	11.76	0.085034014	0.06	16.66666667

adsorption increased from day 2 to day 3 and sudden decrease from day 3 to day 4 and slightly increase in day 5. Similarly, in terms of function of coefficient of the adsorption $\left(\frac{1}{moe^{-rt}}\right)$, increase was observed within the range of 2 to 4 days and sudden decrease in day 5.

The result present in Figure 4 illustrates the adsorption rate of particle size for mango sawdust of 3.35mm in salt water medium upon the influence of time and particle size diameter as well as against the reciprocal of substrate concentration. A lag phase was experienced within 20(g/day)$^{-1}$ to > 20(g/day)$^{-1}$ in terms of functional coefficient of adsorption or reciprocal of specific rate of adsorption as well as reciprocal of the substrate concentration range of 0.085g^{-1} to slightly above 0.085g^{-1}; the illustration defines decrease in reciprocal of maximum specific rate of adsorption with increase in reciprocal of substrate concentration.

The result presented in Table 13 defines the relationship between substrate concentration upon the influence of particle size and time. Increase in substrate concentration was observed with increase in time for particle size of 3.35mm immersed in salt water medium. In terms of the reciprocal of the substrate concentration decrease was observed with increase in time.

Figure 5 illustrates the adsorption rate of particle size of 6.30mm for mango sawdust in salt water medium upon the influence of time. Increase in $\frac{1}{moe^{-rt}}$ was observed with increase in $\frac{1}{S}$ within the range of $\frac{1}{moe^{-rt}}$ = 7.5 to 22(g/day)$^{-1}$ and $\frac{1}{S}$ = >0.08 to <0.0815 as shown in Figure 5.

The results presented in Table 14 illustrate the substrate adsorption concentration upon the influence of time. Increase in substrate adsorbed was experienced with increase in time as well as the reciprocal of the substrate decreases. The rate of adsorption decreased within day 2 to day 3 and remains constant within day 3 to day 4 and suddenly increased from day 4 to day 5 as shown in the Table 14.

The relationship between the reciprocal of maximum functional coefficient of adsorption and the reciprocal of substrate concentration for mango sawdust of particle size of 0.5mm in tap or underground water sample was examined. The result obtained illustrates decrease in the $\frac{1}{moe^{-rt}}$ with increase in $\frac{1}{S}$. The variation in the concentration of $\frac{1}{moe^{-rt}}$ can be attributed to the variation on $\frac{1}{S}$ as presented in Figure 6.

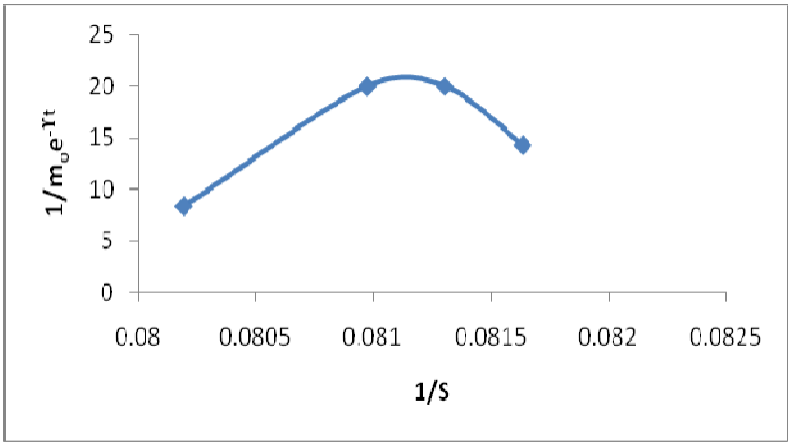

Figure 5. Graph of reciprocal of maximum adsorption rate of particle size (6.30mm) for mango sawdust in salt water against reciprocal of the substrate concentration

Table 14. Rate of adsorption for mango sawdust of particle size 6.30mm in salt water

Day	Substrate (S)	1/ Substrate [S]	Rate of adsorption m_oe^{-rt} (g/day)	Coefficient of adsorption $1/m_oe^{-rt}$ $(g/day)^{-1}$
1	12.18	0.082101806	-	-
2	12.25	0.081632653	0.07	14.28571429
3	12.3	0.081300813	0.05	20
4	12.35	0.08097166	0.05	20
5	12.47	0.080192462	0.12	8.333333333

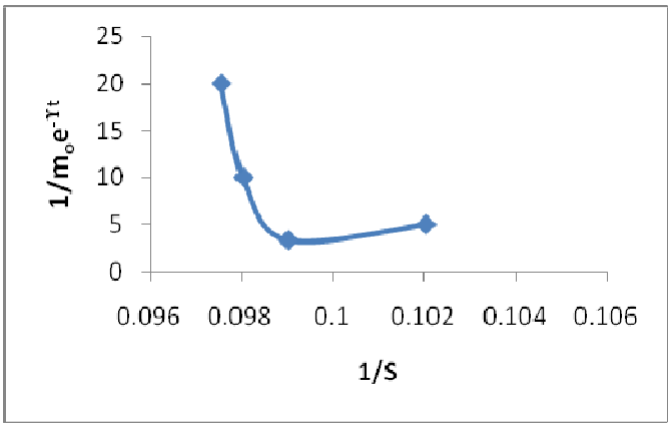

Figure 6. Graph of reciprocal of maximum adsorption rate of particle size (0.5mm) for mango sawdust in tap water against reciprocal of substrate concentration

From Table 15, it is seen that the rate of adsorption of the mango sawdust increases with increase in time. The variation on the rate of adsorption of mango sawdust of particle size of 0.5mm in tap or underground water medium can be attributed to the variation in time. Decrease in the reciprocal of the substrate was observed with increase in time. The rate of adsorption (moe^{-rt}) increased within day 2 to day 3 and decreased within day 3 to day 5 as presented in Figure 15. Similarly, the coefficient of adsorption of $\frac{1}{moe^{-rt}}$ decrease from day 2 to day 3 and suddenly increase from day 3 to day 5.

Figure 7 illustrates the relationship between $\frac{1}{moe^{-rt}}$

Table 15. Rate of adsorption for mango sawdust of particle size 0.5mm in tap water

Day	Substrate (S)	1/ Substrate [S]	Rate of adsorption m_oe^{-rt} (g/day)	Coefficient of adsorption $1/m_oe^{-rt}$ $(g/day)^{-1}$
1	9.6	0.104166667	-	-
2	9.8	0.102040816	0.2	5
3	10.1	0.099009901	0.3	3.333333333
4	10.2	0.098039216	0.1	10
5	10.25	0.097560976	0.05	20

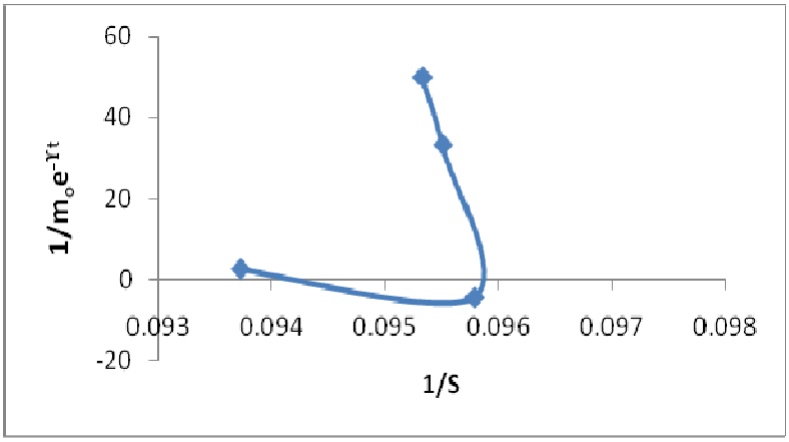

Figure 7. Graph reciprocal of maximum adsorption rate of particle size of (1.18mm) for mango sawdust of in tap water against reciprocal of substrate concentration

Table 16. Rate of adsorption for mango sawdust of particle size 1.18mm in tap water

Day	Substrate(S)	1/ Substrate [S]	Rate of adsorption m_oe^{-rt} (g/day)	Coefficient of adsorption $1/m_oe^{-rt}$ $(g/day)^{-1}$
1	10.3	0.097087379	-	-
2	10.67	0.093720712	0.37	2.702702703
3	10.44	0.095785441	-0.23	-4.347826087
4	10.47	0.095510984	0.03	33.33333333
5	10.49	0.095328885	0.02	50

and $\frac{1}{S}$ upon the influence of particle size of 1.18mm in tap or underground water medium. Decrease in $\frac{1}{moe^{-rt}}$ was observed with increase in $\frac{1}{S}$ as presented in Figure 7. The variation in $\frac{1}{moe^{-rt}}$ can be attributed to the variation in $\frac{1}{S}$ and the curve obtained does not obey the LineWeaver Burk plot, therefore $[Moe^{-rt}]_{max}$ and K_s can not be established.

Table 16 illustrates the rate of adsorption for mango sawdust of particle size of 1.18mm in tap or underground water sample. Increase in adsorption of substrate was observed with increase in time. Similarly, decrease in the reciprocal of the substrate adsorbed was experienced with increase in time. Decrease in rate of adsorption Moe^{-rt} was observed with increase in substrate and time as well as decrease in the reciprocal of the substrate $\frac{1}{S}$. Also decrease in the reciprocal of the functional coefficient of adsorption $\frac{1}{moe^{-rt}}$ with increase in substrate, and time. Decrease in Moe^{-rt} from day 2 to day 3 was experienced and from day 3 to day 5 increase was experienced as presented in Table 16.

Figure 8, illustrates the relationship between $\frac{1}{moe^{-rt}}$

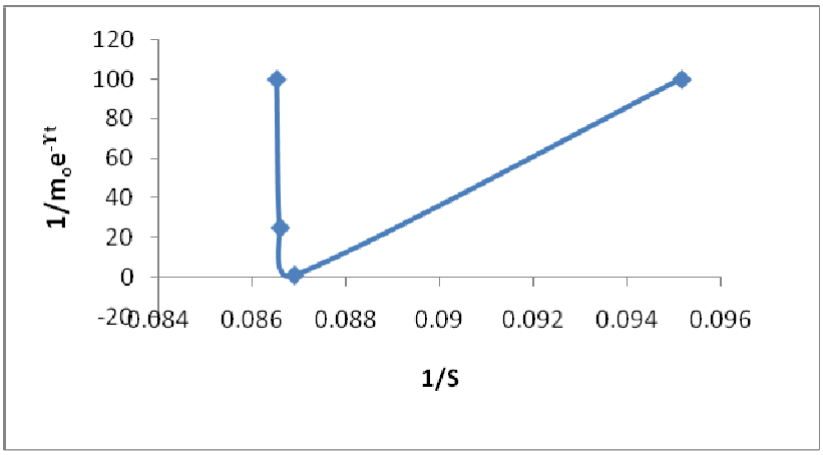

Figure 8. Graph of adsorption rate of particle size of (2.80mm) for mango sawdust in tap water against reciprocal of substrate concentration

Table 17. Rate of adsorption for mango sawdust of particle size 2.80mm in tap water

Day	Substrate(S)	1/ Substrate [S]	Rate of adsorption m_oe^{-rt} (g/day)	Coefficient of adsorption $1/m_oe^{-rt}$ $(g/day)^{-1}$
1	10.5	0.095238095	-	-
2	10.51	0.095147479	0.01	100
3	11.51	0.086880973	1	1
4	11.55	0.086580087	0.04	25
5	11.56	0.08650519	0.01	100

and $\frac{1}{S}$ of particle size of 2.80mm for mango sawdust in tap or underground water sample medium. Decrease in $\frac{1}{moe^{-rt}}$ was observed with increase in $\frac{1}{S}$ and sudden increase was further observed within the range of $\frac{1}{S}$ = > 0.086 > 0.096 as presented in Figure 8. The variation in $\frac{1}{moe^{-rt}}$ can be attributed to variation in $\frac{1}{S}$.

Table 17 illustrates the rate of adsorption for mango sawdust of particle size of 2.80mm in tap water sampled medium. Increase in the rate of adsorption of the substrate was observed with increase in time. The variation on the rate of adsorption of the substrate can be attributed to the variation in time and other functional parameters. Decrease in the reciprocal of the substrate was observed with increase in the as well as the rate of adsorption increased from day 2 to day 3 and suddenly decrease from day 3 to day 5 with increase in time. Similarly, from Table 17, it is seen that $\frac{1}{moe^{-rt}}$ decreases from day 2 to day 3 and suddenly increase from day 3 to day 5 as shown in the paper.

Figure 9 illustrates the relationship between $\frac{1}{moe^{-rt}}$ and $\frac{1}{S}$ for mango sawdust of particle size of 3.35mm in tap water. The variation the concentration of $\frac{1}{moe^{-rt}}$ can be attributed to the variation in $\frac{1}{S}$. Increase in $\frac{1}{moe^{-rt}}$ was experienced within the range of 10 to 100$(g/day)^{-1}$ with the corresponding value of $\frac{1}{S}$ = > 0.086 to > 0.087 as presented in Figure 9.

Table 18 illustrates the rate of adsorption for mango sawdust of particle size 3.35mm in tap water. Increase in the substrate concentration was observed with increase in time. The variation in the rate of adsorption of the substrate can be attributed to the variation in tie and other factors remain the same as discussed above.

Figure 10, illustrates the relationship between $\frac{1}{moe^{-rt}}$ and $\frac{1}{S}$ of particle size of 6.30mm for mango sawdust in tap or underground water sample medium. Decrease in $\frac{1}{moe^{-rt}}$ was observed with increase in $\frac{1}{S}$ and sudden

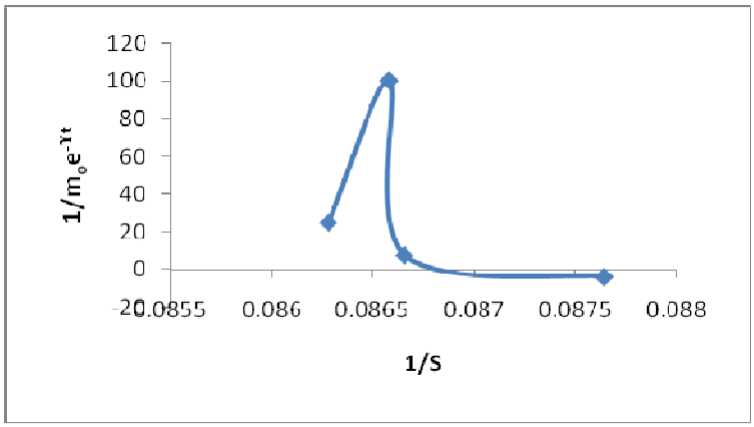

Figure 9. Graph of reciprocal of maximum adsorption rate of particle size 3.35mm of maximum for mango sawdust in tap water against reciprocal of substrate concentration

Table 18. Rate of Adsorption for mango sawdust of particle size 3.35mm in tap water

Day	Substrate (S)	1/ Substrate [S]	Rate of adsorption m_oe^{-rt} (g/day)	Coefficient of adsorption $1/m_oe^{-rt}$ $(g/day)^{-1}$
1	11.68	0.085616438	-	-
2	11.41	0.087642419	-0.27	-3.703703704
3	11.54	0.086655113	0.13	7.692307692
4	11.55	0.086580087	0.01	100
5	11.59	0.086281277	0.04	25

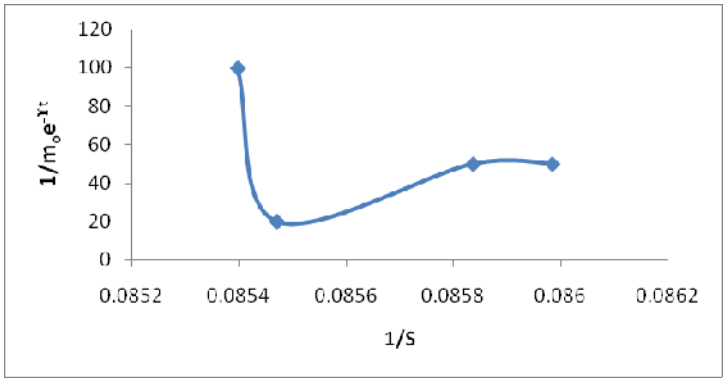

Figure 10. Graph of adsorption rate of particle adsorption for mango sawdust of particle size 6.30mm in tap water against days

increase was further observed within the range of $\frac{1}{S}$ = > 0.0855 > 0.0958 as presented in Figure 10. The variation in $\frac{1}{moe^{-rt}}$ can be attributed to variation in $\frac{1}{S}$.

The results presented in Table 19 illustrate the rate of adsorption for mango sawdust of particle size of 6.30mm in tap water sampled medium. Increase in substrate concentration in terms of adsorption was observed with increase in time. The variation in the substrate concentration was attributed to the variation in time. Decrease in the reciprocal of the substrate was observed with increase in time. The specific rate of adsorption was constant from day 2 to day 3 and increase in day 5 with a sudden decrease from day 4 to day 5.

CONCLUSION

The following conclusions were drawn from the research

Table 19. Rate of adsorption for mango sawdust of particle size 6.30mm in tap water

Days	Substrate(S)	1/ Substrate [S]	Rate of adsorption m_oe^{-rt} (g/day)	Coefficient of adsorption $1/m_oe^{-rt}$ $(g/day)^{-1}$
1	11.61	0.086132644		
2	11.63	0.085984523	0.02	50
3	11.65	0.08583691	0.02	50
4	11.7	0.085470085	0.05	20
5	11.71	0.085397096	0.01	100

work:

(a) In tap H_2O, palm sawdust has the least ability to adsorb oil due to the characteristics of the physicochemical parameters.

(b) In salt H_2O, mango sawdust has the least ability to adsorb oil, this can also be attributed the characteristics of the physicochemical parameters.

(c) Boombas sawdust has the highest rate of adsorption in both salt and tap water among the materials when it was submerged in crude oil polluted water.

(d) There are significant differences in the adsorption abilities among the different oil adsorbents in each set up.

(e) There are significant difference in the adsorption rates between set-up for each oil adsorbent sample

(f) Unfortunately, the graph of $\frac{1}{moe^{-rt}}$ against $\frac{1}{S}$ could not confirm LineWeaver Burk plot principle, hereby resulting to nor determination of $[\frac{1}{moe^{-rt}}]_{max}$ and K_S.

(g) The developed model can be used in predicting and monitoring the rate of adsorption of the used various sawdusts investigated and others.

(h) The composition of the sawdust contributes to the type of microorganisms be isolated and identified

(i) The moisture content, porosity, bulk density and other physicochemical parameters of the sawdust is a major agent that initiates and facilitates the rate of adsorption of various bio-sawdusts.

(j) The various sawdust used, is a major agent or raw material for bioremediation of polluted water environment by crude oil or other liquid chemicals.

REFERENCES

Chaineau CH, Yepremian JF, Vidalie DJ, Ballerini D (2003). 'Bioremediation of crude oil polluted soil: Biodegradation, leaching and toxicity, Water, Air And Soil Pollution Res. 144(1):419-440.

Chorom (2010). "Bioremediation of crude oil-polluted soil by application of fertilizers", Iranian J. Environ. Sci. Engine. Res. 7(4): 347-366.

Kishor KS, Upssana S, Abhimanya Y (2011). Abatement of toxic heavy metals from high way runoff using sawdust as adsorbent, J. Chem. Pharm. Res. 3(1):338-348.

Nwufo BT (1997). Physicochemical studies of the Adsorption of urea and Melamine and sawdust". Niger. J. Chem Res. 2:11-18.

Obidiolayide F, Onuoh AC, Nwachukwu S, Mon C (2010). Bioremediation of crude petroleum stagnant water with fermented cassava step: Report and opinion 2(11):81-86.

Ogoni HA (2001). Development of a mathematical model the optimum Biomas formation in a batch fermentor, Int. J. Model. Simulat. Control (AMSE), 62(3, 4): 46-53.

Omoaghe A (2003). Bioremediation of crude oil polluted soil by the white Rot Fungus, Pleurotos tuberrgium, Environmental Science and Pollution Int. Res. 10(2):108-112.

Omokaro T, Remesh RP (2009). Fungi in Bioremediation of crude oil polluted environments, www.omokaro515@yahoo.com and www.rutwikusa @yahoo.com

Onifade AK, Abubaka FA, Ekundayo FO (2007). Bioremediation of crude oil polluted soil in the Niger Delta Area of Nigeria using enhanced Natural Attenuation, Res. J. Appl. Sci. 2(4):498-504.

Onwuru (1999). Role of diazotrophic bacteria in the bioremediation of crude oil-polluted soil, J. Chem. Technol. Biotechol. Res.74(10):957-964.

Ukpaka CP (2008). Smokeless flare modeling of an associated gas in a production oil fluid J. Model. Simulat. Control (AMSE), 69(1):29-46.

Ukpaka CP (2009). Development of the Biokinetic model for the production of ammonia from Urea in a continuous stirred tank reactor (CSTR). Knowledge Review: A Multidiscipl. J. 19(1):51-74.

Ukpaka CP (2010). Model for the prediction of sulphur Bio-oxidation in Petroleum hydrocarbon in a fluidized bed reactor global research of Engineering and Technology, 3(3):357-370.

Ukpaka CP (2011) Application of Algorithm of Range-Kutta method in Microbial entrained oil recovery in oil wells of Niger Delta in Nigeria. Int. J. Current Res. 3(12):126-132.

Ukpaka CP (2012). Sodium Chloride concentration on the Rheological and Dynamic properties of Aloe-vera Gel. J. Engine.Technol. Res. 4(7):136-148.